Evaluation of the screened Korringa-Kohn-Rostoker method for accurate and large-scale electronic-structure calculations

Rudolf Zeller
Institut für Festkörperforschung, Forschungszentrum Jülich GmbH, D-52425 Jülich, Federal Republic of Germany
(Received 11 November 1996)

The recently proposed concept of a reference system with repulsive, nonoverlapping, spherical potentials as a tool to transform the traditional Korringa-Kohn-Rostoker (KKR) method into a first-principles tight-binding method was investigated numerically. The tests included density-of-states calculations for free space and self-consistent full-potential total-energy calculations for Al, Cu, and Pd. It was found that the densities of states are accurate for energies up to about 3 Ry and that the results for total energies, lattice constants, and bulk moduli excellently agree with the ones obtained by the traditional KKR method. Supercell calculations with up to 500 atoms per unit cell were also done and show that the screened KKR method is advantageous for large-scale density-functional calculations. [S0163-1829(97)01315-5]

I. INTRODUCTION

With the power of modern computers the ability to predict and explain materials properties from first principles by density-functional electronic-structure calculations has improved enormously. For this progress the development of numerical methods and algorithms, however, was at least as important as the computer power. The search for efficient methods, particularly for ones where the computational effort scales linearly with the system size, has recently received much attention.[1–11] Most of these methods are tailored to calculate total energies and forces. They gain their efficiency at the expense of approximations and their range of validity must carefully be studied.[12] Here I want to report investigations for a recently developed tight-binding (TB) version of the traditional multiple-scattering method and to make evident that this version is well suited for large systems, particularly for metallic ones. The transformation into the tight-binding form does not rely on approximations and the resulting screened KKR method has a wide range of applicability.

The multiple-scattering method, originally applied by Lord Rayleigh[13] for sound waves and formulated by Korringa,[14] Kohn and Rostoker[15] for the solution of the Schrödinger equation, has rarely been used for systems with more than a few inequivalent atoms. The problem was mainly the computational complexity caused by long-ranged structure constants, which strongly depend on wave vector and energy. It was shown[16] that these difficulties disappear if one applies an exact screening transformation with suitably chosen screening parameters. These screening parameters are energy dependent, but otherwise similar to the screening constants of the TB-linear-muffin-tin-orbital method.[17] Two different techniques for a straightforward determination of such screening parameters have been developed recently. One technique[18] uses wave function expansions based on unitary spherical waves defined as solutions for a hard sphere solid. The other technique[19] applies a Green-function formulation based on the concept of a reference system with constant repulsive potentials inside nonoverlapping spheres. The Green-function formulation, which is used in this paper, is particularly simple and allows a physically transparent determination of the screening parameters, which are universal in the sense that they do not depend on the geometric arrangement of the spheres. They depend only on energy, the height of the potentials, and the radius of the spheres. It was demonstrated[16,18,19] that the screening transformation can be used to obtain exponentially localized, screened structure constants and it was speculated[16,18,19] that the screened KKR method is well suited to treat large systems. In these systems most of the computational effort involves operations with matrices that are sparse since the screened structure constants can be neglected beyond short distances.

In this paper I want to show that the screened KKR method is very accurate and that it can easily be used for large systems. As illustrative examples I consider free space (the empty-lattice test) as a difficult system for any TB description and self-consistent full-potential total-energy calculations for Al, Cu, and Pd within the local-density approximation of density-functional theory. To demonstrate the usefulness of the method for large systems I also calculated total energies in supercell geometry with up to 500 atoms per unit cell and investigated how well the calculations perform on a massively parallel computer like the Intel Paragon XP/S.

II. THEORY

The Kohn-Sham equations of density-functional theory are usually solved by a choice of basis functions and application of the Rayleigh-Ritz variational principle. Here I use multiple-scattering theory as an elegant alternative. This theory can be formulated in terms of Green functions, which are defined as solutions of

$$[-\nabla_{\mathbf{r}}^2+V(\mathbf{r})-E]G(\mathbf{r},\mathbf{r}',E)=-\delta(\mathbf{r}-\mathbf{r}') \qquad (1)$$

with the appropriate boundary conditions $G(\mathbf{r},\mathbf{r}',E)\rightarrow 0$ for $r\rightarrow\infty$ or $r'\rightarrow\infty$. (I use atomic units $\hbar^2/2m=1$.) Here $V(\mathbf{r})$ denotes the density-functional effective potential and E the

energy. The Green functions for two different potentials $V(\mathbf{r})$ and $V^r(\mathbf{r})$ are connected by a Dyson equation

$$G(\mathbf{r},\mathbf{r}',E)=G^r(\mathbf{r},\mathbf{r}',E)+\int G^r(\mathbf{r},\mathbf{r}'',E) \times[V(\mathbf{r}'')-V^r(\mathbf{r}'')]G(\mathbf{r}'',\mathbf{r}',E)d\mathbf{r}'', \quad (2)$$

which can be verified by applying the operator $-\nabla^2_{\mathbf{r}}+V^r(\mathbf{r})-E$ on both sides of (2). The underlying principle for the screening transformation is the freedom in the choice of the reference potential $V^r(\mathbf{r})$. In the original KKR method the reference system is free space. This has the advantages that the reference potential $V^0(\mathbf{r})$ vanishes and that the reference Green function is analytically known as

$$G^0(\mathbf{r},\mathbf{r}',E)=-(4\pi|\mathbf{r}-\mathbf{r}'|)^{-1}\exp(iE^{1/2}|\mathbf{r}-\mathbf{r}'|), \quad (3)$$

where superscript 0 refers to free space. On the other hand, it is well known that the free-electron band structure is responsible for the singularities in the KKR structure constants, which are difficult to evaluate because of their complicated wave vector and energy dependencies.

These difficulties can be removed by a reference system, in which all bands are shifted to higher energies. The choice of a constant repulsive potential in all space would simply move the zero of the energy scale and allow us to do the density-functional calculations at negative energies, for which according to (3) the Green function decays exponentially. This simple choice, however, leads to difficulties if one wishes to apply multiple-scattering theory to solve the integral equation (2) with the help of linear algebraic equations given by (5) below.

In multiple-scattering theory the Green function can be written[20] in cell centered coordinates such as

$$G(\mathbf{r}+\mathbf{R}^n,\mathbf{r}'+\mathbf{R}^{n'},E)=\delta^{nn'}G_s(\mathbf{r}+\mathbf{R}^n,\mathbf{r}'+\mathbf{R}^n,E) +\sum_{LL'}R^n_L(\mathbf{r},E)G^{nn'}_{LL'}(E)R^{n'}_{L'}(\mathbf{r}',E), \quad (4)$$

where $\mathbf{R}^n$ denotes the centers of atomic and possibly empty cells and $\mathbf{r}$ the vectors within the cells. $L=(\ell,m)$ stands for the angular momentum numbers and $R^n_L(\mathbf{r},E)$ and $G_s(\mathbf{r}+\mathbf{R}^n,\mathbf{r}'+\mathbf{R}^n,E)$ are wave functions and the Green function for a single potential restricted to the Voronoi cell, which surrounds the position $\mathbf{R}^n$. The structural Green-function matrix elements $G^{nn'}_{LL'}(E)$ are determined by

$$G^{nn'}_{LL'}(E)=G^{r,nn'}_{LL'}(E)+\sum_{n''}\sum_{L''}G^{r,nn''}_{LL''}(E) \times\sum_{L'''}[t^{n''}_{L''L'''}(E)-t^{r,n''}_{L''L'''}(E)]G^{n''n'}_{L'''L'}(E), \quad (5)$$

where $t^n_{LL'}(E)$ and $t^{r,n}_{LL'}(E)$ are the usual t matrices for the potentials $V(\mathbf{r})$ and $V^r(\mathbf{r})$ restricted to the cell at $\mathbf{R}^n$.

The disadvantage of a constant repulsive potential in all space is the difficult determination of the single-site quantities $R^n_L(\mathbf{r},E)$ and $t^n_{LL'}(E)$. A potential, which is constant inside an atomic cell and vanishes outside, requires a complicated full-potential KKR treatment because of the faceted shape of the cell. Although such calculations are now commonly assumed to be possible,[20–23] the question of angular momentum convergence is still under debate.

The reference system recently suggested by Zeller *et al.*[19] does not suffer from these problems. It avoids the difficulties of a full-potential KKR treatment by the choice of muffin-tin potentials, which are easily implemented into existing KKR computer programs, and does not require higher angular momenta than the standard KKR method. The only added work consists in the determination of the structural Green-function matrix elements $G^{r,nn'}_{LL'}(E)$ for the reference system. Whereas the elements $G^{0,nn'}_{LL'}(E)$ for free space are analytically known as sums over combinations of Hankel functions and spherical harmonics, the elements $G^{r,nn'}_{LL'}(E)$ for an arbitrary reference system are calculated numerically. The equation to be solved has the form

$$G^{r,nn'}_{LL'}(E)=G^{0,nn'}_{LL'}(E) +\sum_{n''}\sum_{L''}G^{0,nn''}_{LL''}(E)t^{r,n''}_{\ell''}(E)G^{r,n''n'}_{L''L'}(E), \quad (6)$$

which is similar to (5) with the simplification that the t-matrix t^0 of free space vanishes and that the t-matrix $t^{r,n}_{LL'}(E)=t^{r,n}_{\ell}(E)\delta_{LL'}$ is diagonal in the angular-momentum indices as a consequence of the nonoverlapping spherical potentials in the reference system. The matrix elements $G^{r,nn'}_{LL'}(E)$ represent the TB parameters in the screened KKR method and decay exponentially with the distance between $\mathbf{R}^n$ and $\mathbf{R}^{n'}$ if the reference potentials are repulsive enough and the energies are not too high.[19] It is important that the exponential decay allows us to restrict the sum over n'' in (6) to a finite number of sites around $\mathbf{R}^{n'}$. It is also useful that (6) can be solved independently for each site n and for each energy E. Thus the solution is suitable for massively parallel computing and the effort to obtain the TB parameters $G^{r,nn'}_{LL'}(E)$ scales linearly with the number of sites n in the system, for which one wishes to calculate the electronic structure.

For the numerical accuracy and efficiency of the screened KKR method, an interesting question is how many sites n'' must be taken into account in (6) and how the necessary number of sites depends on the height of the repulsive potentials. It would be desirable to have TB parameters $G^{r,nn'}_{LL'}(E)$, which decay fast enough so that only nearest or perhaps next nearest neighbors n' of site n are needed to determine these TB parameters by solving (6). In the subsequent solution of (5) the short-ranged TB parameters lead to sparse matrices for large systems since only nearby sites are coupled. If the sparsity is efficiently exploited, large-scale density-functional calculations within the screened KKR method should become possible.

III. ACCURACY

A. Densities of states for free space

It is well known that the standard KKR method fulfills the empty-lattice test for the vanishing potential[24] and gives the

exact band structure and the exact density of states (DOS) for free space. If the TB parameters of the screened KKR method are obtained in real space by restricting the sum over n'' in (6) to a finite cluster of sites, this approximation cannot give the exact DOS. Nevertheless, the error can be expected to be small if the TB parameters decay fast enough and if enough sites are used in (6). To assess the size of the error, I have solved (6) for different numbers of sites with potentials of various height and used the obtained TB parameters to calculate the DOS of free space using an empty fcc lattice with a lattice constant of 361.50 pm.

For a periodic arrangement the solution of (5) contrary to (6) involves an infinite number of sites n'' and was achieved by lattice Fourier transform and subsequent Brillouin-zone (BZ) integration. The structural Green-function elements $G_{LL'}^{r,nn'}(E)$ are easily Fourier transformed by

$$G_{LL'}^{r,\mu\mu'}(\mathbf{k},E)=\sum_{m'} \exp(i\mathbf{k}\mathbf{R}^{m}-i\mathbf{k}\mathbf{R}^{m'})G_{LL'}^{r,nn'}(E), \quad (7)$$

where $\mathbf{R}^m$ and $\mathbf{R}^\mu$ denote the translation vectors of the lattice and the basis vectors in the unit cell. The atomic positions are then given by $\mathbf{R}^n=\mathbf{R}^m+\mathbf{R}^\mu$. The sum (7) over all lattice translation vectors converges fast because the terms decay exponentially, whereas the standard $\mathbf{k}$ space structure constants $G_{LL'}^{0,\mu\mu'}(\mathbf{k},E)$ usually require Ewald summations.[25] For the BZ integrations I used a straightforward sampling on a uniform grid and exploited the cubic symmetry of the grid points as described by Blöchl *et al.*[26] The direct sampling naturally causes more noise than a sophisticated analytical integration scheme like the tetrahedron method, in particular for higher energies. Nevertheless, the direct sampling was chosen because it was more advantageous for the large supercells considered in Sec. IV. For the DOS calculations I reduced the BZ sampling noise by a large number of 11 726 symmetry inequivalent points and by an artificial broadening. The broadening reflects a finite temperature T and is achieved by complex energies E with an imaginary part $\pi kT=0.21$ eV, which corresponds to $T=800$ K, the temperature used in the self-consistent calculations in Sec. III B. I used repulsive potentials of 2, 4, and 8 Ry height within the muffin-tin spheres of the fcc lattice and clusters consisting of 13, 19, 43, and 79 potentials at neighboring sites of the fcc lattice. With 16 angular momentum components, corresponding to $\ell_{\max}=3$, the matrix dimensions in (6) were 204, 304, 688, and 1264. For the solution of the linear equations I used efficient computer codes,[27] which are now available on a variety of computers.

The density of states was obtained from the Green function (4) by integrating the imaginary part of $G(\mathbf{r},\mathbf{r},E)$ over the Wigner-Seitz cell of the fcc lattice. Figure 1(a) shows the results as a function of energy calculated with TB parameters obtained from a cluster with 79 repulsive potentials. For comparison the exact result is also shown. The curves follow the familiar square root behavior except for a small broadening near $E=0$ as a consequence of the imaginary part of E. The screened KKR results agree with the exact one for lower energies, for higher energies they suddenly deviate and can also have unphysical, negative values. For still higher energies, they may become positive again, but these meaningless

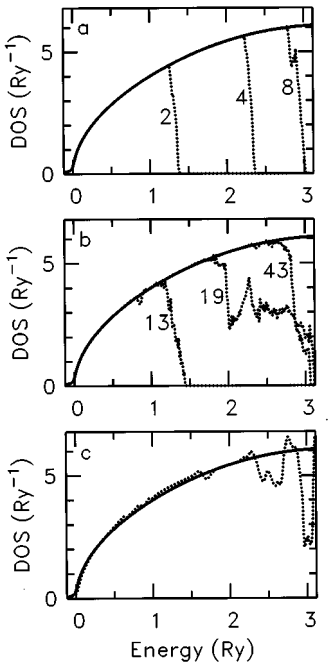

FIG. 1. Density of states (DOS) for free space. Broken lines refer to screened KKR calculations, solid lines to the exact result. (a) The numbers indicate the height (in units of Ry) of the 79 repulsive potentials used to determine the TB parameters. (b) The numbers indicate how many repulsive potentials of height 8 Ry were used to determine the TB parameters. (c) The TB parameters were obtained with 79 repulsive potentials of 8 Ry height, but only the nearest-neighbor parameters were used in the DOS calculation.

values are not shown in Fig. 1. The energy range where the screened KKR method is applicable becomes larger for higher potentials and the sudden breakdown arises when the TB parameters $G_{LL'}^{r,nn'}(E)$ begin to decay so slowly that solving (6) in real space makes no sense. It is satisfying that accurate DOS values can be calculated almost up to energies of 3 Ry. Thus the screened KKR method works well not only for occupied, but also for unoccupied states provided that the energy is not too high. Consequently, meaningful comparisons of spectroscopic measurements like inverse photoemission, near-edge x-ray absorption, and magnetic x-ray dichroism with calculated densities of states and related quantities are possible within the screened KKR method. The close agreement of the results at lower energies for different heights indicates that no angular momentum convergence problems appear even for 8 Ry high potentials.

Figure 1(b) shows the free space DOS calculated by using different numbers of repulsive potentials. The energy range where the screened KKR method is applicable becomes larger if more repulsive potentials are used. For energies up to about 1 Ry the use of 13 or 19 repulsive potentials seems to be enough. Only these energies appear in the self-consistent calculations of Sec. III B.

For large-scale calculations, an interesting question is whether better nearest-neighbor TB parameters $G_{LL'}^{r,nn'}(E)$ can be obtained for use in (5) if they are calculated with repulsive potentials, which are not restricted to nearest-neighbor sites. Compared to the result in Fig. 1(b) for 13 potentials an overall improvement is seen in Fig. 1(c) where

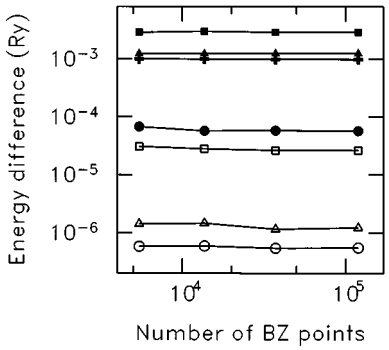

FIG. 2. Total energy differences between screened and standard KKR results for Al as function of the number of sampling points in the full Brillouin zone. Crosses refer to 19 repulsive potentials used for the determination of the TB parameters. Full squares, triangles, and circles refer to 13, 43, and 55 potentials, open squares, triangles, and circles to 79, 153, and 225 potentials.

the nearest-neighbor TB parameters were obtained with 79 repulsive potentials. The energy range, where the screened KKR method gives a reasonable DOS, increases, but some small systematic deviations already appear for lower energies. The reason for these discrepancies is not yet clear and requires further investigation beyond the scope of the present paper.

B. Total energies for Al, Cu, and Pd

In this section I want to assess the precision of the screening transformation for self-consistent total-energy calculations for Al, Cu, and Pd as typical examples for simple, noble, and transition metals. The total energies were calculated by a full-potential version of multiple-scattering theory[20,28] with $\ell_{\max}=3$ as the highest angular momentum for wave functions, t matrices, and structural Green-function elements and with $\ell_{\max}=6$ for charge densities and potentials. Integrations over Wigner-Seitz cells were done by using shape truncation functions.[29] The calculations were nonrelativistic and the exchange-correlation potential of Ceperley and Alder[30] was applied in the parametrization of Vosko, Wilk, and Nusair.[31] The fundamental quantity of density-functional theory, the electron density was determined from (4) by a complex-energy integral[32] using a finite-temperature contour.[33] The contour consisted of three straight lines as described by Zeller[34] with eleven Gaussian integration points and of five Matsubara frequencies starting with $\mu+i\pi kT$. Here μ is the chemical potential and πkT is chosen as 0.21 eV, which corresponds to a temperature of 800 K.

Figure 2 displays total-energy differences between standard and screened KKR calculations for Al. The TB parameters were determined from clusters with different numbers of repulsive potentials of 8 Ry height. The results as well as similar results for Cu and Pd show little dependence on the number of points used for the BZ integration. This independence can be explained by the fact that the equivalence of (5) and (6) with the standard KKR equation $G=G^0+G^0tG$ remains valid under Fourier transformation. A detailed account of the total-energy differences is given in Table I. For TB parameters determined from (6) with 153 or 225 repulsive potentials, the total energies differ less than 1 μRy from the values of standard KKR calculations. For 225 potentials of 2 or 4 Ry height the total energies even agree within 0.1 μRy. This means that total energies, for which the standard KKR values were calculated as $-482.937\,890\,35$, $-3275.896\,685\,31$, and $-9871.014\,493\,09$ Ry for Al, Cu, and Pd, can be obtained with a relative precision of 10^{-10}. This precision is very satisfactory and assures that both screened and standard structure constants were calculated with high accuracy. The close agreement within 1 μRy between screened and standard KKR total energies also demonstrates that no angular momentum convergence problems occur if the components of the t matrix of the reference system are neglected in (5) and (6) beyond $\ell_{\max}=3$. The agreement also establishes that the screening transformation accurately works in the complex energy plane, whereas the DOS results in Sec. III A could only prove the validity of the screening transformation for real energies. The total energies do not much depend on the height of the potentials and considerably improve if 55 instead of 43 repulsive potentials are used to determine the TB parameters. The inclusion of all

TABLE I. Total-energy differences ΔE between standard and screened KKR calculations. The first row contains the number of repulsive potentials of height V^r which were used to determine the TB parameter. The BZ integrations were done with 891 symmetry inequivalent points corresponding to 37 288 points in the full zone.

No. of potentials		13	19	43	55	79	153	225
	V^r (Ry)	(mRy)	(mRy)	(mRy)	ΔE (μRy)	(μRy)	(μRy)	(μRy)
Al	2	6.39	0.99	0.08	−15.2	6.3	−0.27	0.05
	4	−0.19	−0.19	0.53	37.3	10.8	0.52	0.11
	8	−2.88	−0.98	1.24	57.7	26.2	1.14	0.53
Cu	2	−0.48	2.28	0.32	6.4	−13.9	−0.67	−0.03
	4	−3.38	0.62	0.28	−20.5	0.0	−0.07	0.06
	8	−3.89	0.55	0.51	−24.0	−1.0	0.11	0.34
Pd	2	−0.66	0.93	0.55	14.4	1.1	−0.18	0.06
	4	−1.84	0.59	0.63	−3.0	−1.9	−0.03	0.11
	8	−1.77	1.10	1.07	8.8	0.6	0.25	0.33

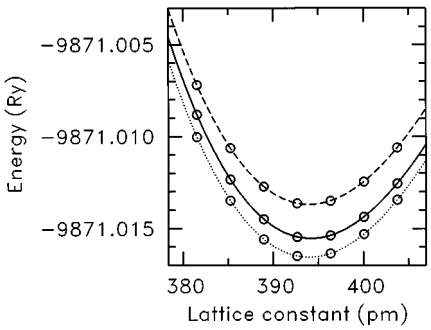

FIG. 3. Total energies for Pd as a function of the lattice constant. The BZ integrations were done with 891 symmetry inequivalent points. Dashed, dotted, and solid lines refer to 13, 19, and 55 potentials of 8 Ry height which were used to determine the TB parameters. The standard KKR result is indistinguishable from the solid line.

second neighbors in the 110 directions is thus important if accurate TB parameter are required.

If moderate mRy accuracy is wanted, nearest-neighbor couplings (13 sites) are enough in (6) and (5) for the determination of TB parameters and structural Green-function elements. This short coupling range is a property in the repulsive reference system alone. In this respect the screened KKR method is clearly distinguished from most $O(N)$ methods suggested in the literature,[1–11] for which the coupling range in the studied materials should be short and is exploited. For metallic systems with longer-ranged couplings the screened KKR method is thus particularly useful.

It is important to investigate how the total-energy errors given in Table I affect derived quantities like lattice constants and bulk moduli. For that purpose I calculated the total energies for seven lattice constants and fitted the results to a Birch-Murnaghan equation of state[35] in the form

$$E_{tot}=\sum_{m=1}^{4} c_m a^{4-2m}, \tag{8}$$

where a is the lattice constant and c_m are the fitting parameters. Figure 3 shows for Pd that the fits are nearly perfect and similarly good fits were also found for Al and Cu. No differences of the fitted curves with the calculated points can be seen. From the derivatives of (8) with respect to a, I obtained the numerical values for the lattice constants and bulk moduli given in Table II. I checked the adequacy of the uniform BZ sampling by using 2736 points instead of 891. The larger number changes the lattice constants by less than 0.02% and the bulk moduli by less than 0.5%. The results in Table II clearly show that nearest-neighbor TB parameters are enough if one wishes to calculate lattice constants with pm accuracy and bulk moduli with GPa accuracy.

Contrary to the total energy other electronic properties are not protected by density-functional stationary properties and one may expect that they cannot be calculated with similar accuracy. This is indeed true as Table III shows where angular-momentum decomposed charges are given. With TB parameters obtained from 13 repulsive potentials the error is of the order of 10^{-2} and from 19 repulsive potentials of the order of 10^{-3} electrons. The latter value seems to be accurate enough for practical purposes. With enough repulsive potentials, of course, the standard and screened KKR results agree much better. Table III shows deviations of several 10^{-5} electrons for 79 repulsive potentials and I found that only the last digit of the charges deviates from the results of standard KKR calculations if I used 153 or 225 repulsive potentials to determine the TB parameters.

Concluding this section I want to point out that different quantities converge differently with respect to the number of repulsive potentials used to determine the TB parameters. Total energies, lattice constants, and bulk moduli were easily calculated with a high accuracy, angular momentum decomposed charges were moderately more difficult to obtain, and DOS calculations at higher energies demanded rather accurate TB parameters.

IV. SUITABILITY FOR LARGE-SCALE CALCULATIONS

The main computational tasks consist in the calculation of single-site quantities like $R_L^n(\mathbf{r},E)$ and $t_{LL'}^n(E)$ and of the structural Green-functions $G_{LL'}^{nn'}(E)$. The single-site quantities can be calculated independently for each site with $O(N)$ operations. Here N denotes the number of sites in the system, for which one wishes to calculate the electronic structure. The direct solution of (5) for nonsparse matrices requires $O(N^3)$ operations and dominates the computational effort for large systems.

The screened KKR method applies rather sparse matrices G^r, particularly if only nearest-neighbor couplings are used, which according to Sec. III B yield good values for total energies, lattice constants, and bulk moduli. Substantial savings of computer time and storage can be expected if (5) is

TABLE II. Lattice constants a and bulk moduli B_0 for Al, Cu, and Pd determined by standard and screened KKR calculations. The potentials used to obtain the TB parameters were 8 Ry high. The BZ integrations were done with 891 symmetry inequivalent points corresponding to 37 288 points in the full zone.

No. of	Al		Cu		Pd	
potentials	a (pm)	B_0 (GPa)	a (pm)	B_0 (GPa)	a (pm)	B_0 (GPa)
13	402.22	80.69	358.52	165.41	393.97	178.33
19	401.08	80.64	358.02	170.83	393.97	179.48
43	400.96	81.21	358.18	168.91	394.02	180.22
79	400.93	81.49	358.20	169.68	394.16	178.82
Standard	400.93	81.47	358.20	169.63	394.16	178.78

TABLE III. Amount of s, p, and d charge within the Wigner-Seitz unit cell for Al, Cu, and Pd determined by standard and screened KKR calculations. The potentials used to obtain the TB parameters were 8 Ry high. The BZ integrations were done with 891 symmetry inequivalent points corresponding to 37 288 points in the full zone.

No. of potentials		13	19	79	Standard
Al	s	1.146521	1.141920	1.140812	1.140898
	p	1.443042	1.433167	1.432605	1.432586
	d	0.394480	0.404844	0.405439	0.405372
Cu	s	0.683831	0.679906	0.679554	0.679516
	p	0.707896	0.711790	0.710796	0.710803
	d	9.554109	9.552431	9.553584	9.553614
Pd	s	0.553231	0.552433	0.550710	0.550706
	p	0.576841	0.577796	0.578144	0.578099
	d	8.757122	8.756274	8.758072	8.758135

solved by sparse matrix techniques.[36,37] For problems like surfaces, interfaces, and thin films the two-dimensional periodicity allows us to remove two of the three space dimensions and direct solution methods for (5) with $O(N)$ complexity exist. An $O(N)$ algorithm was recently implemented to develop a slab program and is the subject of a separate paper.[38] For general three-dimensional problems the decision, whether direct or iterative solution methods should be preferred, is not trivial. Available standard algorithms, in particular, the iterative ones, often require positive definiteness of the matrices, whereas G^r is not even Hermitian, and these algorithms usually do not exploit the block-sparse structure of G^r. The search for good algorithms, perhaps using physically based ideas like the recursion technique,[39] remains a subject of future research and is beyond the scope of the present paper. For the large-scale calculations described below it was my purpose to demonstrate that they can already be done by the screened KKR method without the use of sparsity.

A. Supercell total energies

The application of the standard KKR method to large unit cells has been prevented in the past by the complicated structure constants and the difficult search for zeros of the KKR determinant, which are necessary to obtain the band structure. This process requires $O(N^4)$ operations. The Green-function formulation of Sec. II with complex-energy integration allows us to determine the electronic density without the knowledge of the band structure. In this formulation only linear equations must be solved and the operation count is reduced to $O(N^3)$, but in the standard KKR method the complicated structure constants remain. Contrary to that the screened KKR method applies a simple Fourier transform (7) to calculate the necessary matrices from the TB parameters. This is the main simplification, which I exploited for the calculations with 4, 32, 108, 256, and 500 atoms per supercell. My interest was to investigate how many points in the Brillouin zone one needs to obtain total energies with an accuracy of several μRy per atom. Chetty *et al.*[40] argue that such accuracies are required if supercells with about 100 atoms are used, for instance, to determine vacancy formation energies with a precision of 0.01 eV.

For the supercell calculations I applied a potential taken from standard KKR calculations obtained with 11 726 symmetry inequivalent BZ sampling points. Because the density-functional total energy is stationary with respect to the potential taken as a trial quantity,[41] one expects that self-consistency is not needed for accurate total energies. I checked the effect of self-consistency and found that the total energies do not change, at least for the larger numbers of BZ points, which were the target of my investigation. For the calculations I solved only (5) in supercell geometry with the atoms being on fcc lattice positions with the experimental fcc lattice constants given by 404.96, 361.50, and 388.98 pm for Al, Cu, and Pd. The supercell electronic density is thus identical for all atoms and was used to calculate the total energy, in particular its Coulomb part, in fcc geometry. In this way the supercell size effect on the solution of (5), which is influenced by the number of BZ points, was clearly separated from size effects on Poisson's equation which were not considered.

Chetty *et al.*[40] suggest and show that the product of the number K of BZ points and the number N of atoms per supercell is the quantity, which decides the accuracy of supercell calculations. The calculated screened KKR total energies for Cu are shown in Fig. 4 where the results are plotted as differences from the converged result which was obtained with $N=4$ and 4960 symmetry inequivalent sam-

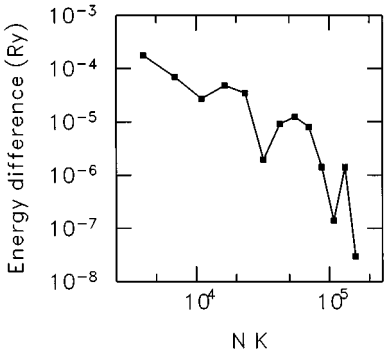

FIG. 4. Screened KKR total energies for Cu as function of the product of the number N of atoms in the supercell and of the number K of sampling points in the Brillouin zone. The energies are given as differences from the converged result for $NK\rightarrow\infty$.

pling points corresponding to $K=216\,000$. The TB parameters were obtained from 79 repulsive potentials of 4 Ry height and the largest system treated was a supercell with 500 atoms and 10 symmetry inequivalent sampling points corresponding to $K=216$. The total energies for different sizes of the supercell and identical values of NK always agreed better than 10^{-8} Ry indicating that no numerical instabilities occurred in the algorithms used for the large-scale calculations. From a computing point of view the screened KKR method uses only standard linear algebra software. Thus it is more simply applied than the sophisticated iterative techniques which Chetty *et al.*[40] used to save computer time and storage.

B. Computational aspects

Whereas most $O(N)$ techniques suggested recently[1–11] suffer from a large calculational overhead if less than about 100 inequivalent atoms are treated, the screened KKR method becomes competitive with the standard KKR method already for small systems. This is true not only for layered systems as discussed by Zeller *et al.*[19] and Wildberger *et al.*,[38] but also for general three-dimensional systems. If the possible sparsity of the matrix G^r is not used, the screened KKR method differs from the standard one only in the evaluation of structure constants. Identical tasks calculate the single-site t matrices and wave functions, obtain the density from the structural Green-function elements and determine the potential from the density by Poisson's equation. Whereas the standard structure constants are obtained by Ewald summations, the screened structure constants are obtained by a simple Fourier transform (7) from the **k** independent TB parameters $G_{LL'}^{r,nn'}(E)$. Thus the work for each **k** point is smaller in the screened KKR method. For instance, to obtain a specified μRy precision for the total energies of Sec. III B, I used 1.6 s of computing time per BZ point with the standard KKR method and only 0.08 s with the screened one (on a workstation IBM RS/6000 model 3CT). The **k** independent overhead is 27 s for the standard method and 260 s for the screened one. The latter time refers to the determination of TB parameters for a cluster of 79 repulsive potentials if group theory is utilized to exploit the cubic symmetry of the cluster. This means that the screened KKR calculations for a fcc unit cell with *one* inequivalent atom were already faster for more than about 150 **k** points.

The large supercell calculations were possible by mainly three reasons. The matrix dimensions given by 16 times the number of atoms (for $\ell_{\max}=3$) are economic, efficient linear equation solvers[27,42] exist on a variety of computers, and powerful vector and parallel computers like the CRAY T90 and the Intel Paragon XP/S 10 were available. I applied the supercomputers mainly because of the large memory needed to store the full structural Green-function matrix G^r for 256 or 500 atoms, whereas I could treat supercells with up to 108 atoms on a workstation. The efficiency of the available linear equation solvers can be judged from the computing rates given in Table IV, which were estimated using an operation count of $8n^3$ where n denotes the dimension of the complex matrices. The measured operation counts on the CRAY T90 agreed with the estimated ones within one percent indicating that the time to calculate the matrix elements is negligible.

TABLE IV. Computing rates in units of 10^9 floating point operations per second for various numbers N of atoms in the supercell. The number of processors p used on the Intel Paragon is given in the last column.

N	IBM	CRAY	Intel	p
32	0.186	1.03	0.38	16
108	0.217	1.39	2.40	81
256		1.53	2.95	64
500		1.56	4.90	100

Table IV shows that the workstation delivers up to 82% of its peak rate of 0.264 Gflops and the vector computer up to 87% of its peak rate of 1.8 Gflops.

C. Parallel computing

Since fast vector computers are expensive, an interesting question is whether cheaper massively parallel computers can efficiently be applied to solve (5). In the Green-function formulation of the KKR method several parallelization strategies are possible. A simple strategy distributes the work according to the complex-energy integration mesh points. Already for the standard KKR method this energy parallelization performs well[43] in spite of the complicated determination of the structure constants. For the screened KKR method almost perfect performance can be expected. For large systems this strategy has two disadvantages. Large storage memories are necessary on the processors and not more than about 20 processors can be used because not more energy mesh points are usually required to determine the electronic density in self-consistent calculations. Therefore I investigated a different strategy, which distributes the matrix G^r and solves each linear system (5) with the participation of all processors. Because of the simple Fourier transform (7) the distributed parts of G^r were straightforwardly obtained in parallel. The combined use of all processors to solve (5) was facilitated by a standard software package,[42] which recently became available.

Figure 5 shows the speedup, which I obtained for various supercell sizes and a number of processors. The calculations for 108 atoms covered the widest range from four to 81

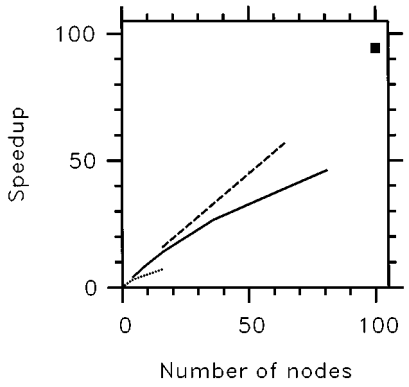

FIG. 5. Speedup as function of the number of nodes for 108 atoms per supercell (solid line). The square and the dashed and dotted lines refer to 500, 256, and 32 atoms assuming that the computing time scales with the cube of the number of atoms.

processors. A single processor had not enough memory and thus the speedup values are scaled by arbitrarily assuming a speedup of four for four processors. For 256 and 500 atoms even four processors could not be used. For these supercell sizes the computing time necessary on four processors was estimated by scaling the time measured for 108 atoms with the cube of the number of atoms, essentially in agreement with the operation counts given by the CRAY T90.

Figure 5 shows a satisfactory speedup, for instance more than 50% efficiency was achieved with 81 processors for 108 atoms, 90% efficiency with 64 processors for 256 atoms, and 95% efficiency with 100 processors for 500 atoms. For a fixed number of atoms the speedup saturated with the number of processors, whereas a simultaneous increase of the numbers of processors and atoms was highly efficient. I want to point out that both strategies, distributing the matrix and parallelizing the complex-energy points, can be applied together. For that reason several hundred processors can be expected to be useful for screened KKR calculation. I also want to remark that the calculation of the single-site quantities can also be doubly parallelized with respect to sites and energy mesh points.

V. SUMMARY

I have investigated the screened KKR method based on the concept of a reference system with repulsive, nonoverlapping, spherical potentials as a tool for TB electronic-structure calculations. The calculated results for densities of states, angular momentum decomposed charges, total energies, lattice constants, and bulk moduli demonstrate that the screened KKR method is very accurate. The TB parameters can be calculated in real space using a finite cluster of repulsive potentials. The results for densities of states improve with cluster size and potential height. If the potentials are chosen high enough, for instance, higher than 2 Ry, the height has minor consequences for angular momentum decomposed charges and little effect on total energies, lattice constants, and bulk moduli. With nearest-neighbor TB parameters, obtained from only 13 repulsive potentials, the bulk moduli and the lattice constants could be determined within 1 GPa and 0.1 pm. Comparable accuracy can be expected for similar quantities like other elastic constants, phonon properties, and determinations of geometrical arrangements.

The screened KKR method introduces little computational overhead compared to the standard KKR method and situations exist where the screened KKR method is faster even for one atom per unit cell. The effort to implement the screening transformation into existing KKR computer programs is small and the computations mainly require solutions of linear algebraic equations, for which efficient standard software exists. Due to the economic matrix dimensions the screened KKR method is suitable for large-scale calculations on workstations and on supercomputers. Parallelization is simply possible with respect to the complex-energy integration mesh points. For each mesh point further parallelization is possible for the single-site quantities and for the solution of large linear equations.

It can be expected that the screened KKR method routinely allows large-scale density-functional calculations in the future if the sparsity of the matrices can efficiently be exploited. For layered systems good algorithms with $O(N)$ complexity already exist. Compared to other recently suggested $O(N)$ methods the screened KKR method is directly applicable for metallic systems and for density-of-states calculations, which can be compared to spectroscopic experiments like inverse photoemission, near-edge x-ray absorption, and magnetic x-ray dichroism.

ACKNOWLEDGMENTS

It is a pleasure to thank P. H. Dederichs for many helpful discussion. The work has benefited from collaborations within the HCM Network Contract No. ERBCHRXCT930369 and the TMR Network Contract No. EMRX-CT96-0089. Part of the calculations were done on the CRAY T90 and Intel Paragon XP/S 10 computers of the Forschungszentrum Jülich.

[1] M. Krajci and J. Hafner, Phys. Rev. Lett. **74**, 5100 (1995).
[2] Y. Wang, G. M. Stocks, W. A. Shelton, D. M. C. Nicholson, Z. Szotek, and W. M. Temmerman, Phys. Rev. Lett. **75**, 2867 (1995).
[3] I. A. Abrikosov, A. M. N. Niklasson, S. I. Simak, B. Johansson, A. V. Ruban, and H. L. Skriver, Phys. Rev. Lett. **76**, 4203 (1996).
[4] S. Wei and M. Y. Chou, Phys. Rev. Lett. **76**, 2650 (1996).
[5] T. Zhu, W. Pan, and W. Yang, Phys. Rev. B **53**, 12 713 (1996).
[6] S. Goedecker and L. Colombo, Phys. Rev. Lett. **73**, 122 (1994); A. F. Voter, J. D. Kress, and R. N. Silver, Phys. Rev. B **53**, 12 733 (1996).
[7] A. P. Horsfield, A. M. Bratkovsky, M. Fearn, D. G. Pettifor, and M. Aoki, Phys. Rev. B **53**, 12 694 (1996).
[8] S. Itoh, P. Ordejon, D. A. Drabold, and R. M. Martin, Phys. Rev. B **53**, 2132 (1996).
[9] E. Hernandez, M. J. Gillan, and C. M. Goringe, Phys. Rev. B **53**, 7147 (1996).
[10] A. Canning, G. Galli, F. Mauri, A. De Vita, and R. Car, Comput. Phys. Commun. **94**, 89 (1996).
[11] Further information on work for $O(N)$ methods may be found in Refs. 1–10.
[12] K. C. Pandey, A. R. Williams, and J. F. Janak, Phys. Rev. B **52**, 14 415 (1995).
[13] Lord Rayleigh, Philos. Mag. **34**, 481 (1892).
[14] J. Korringa, Physica **13**, 392 (1947).
[15] W. Kohn and N. Rostoker, Phys. Rev. **94**, 1111 (1954).
[16] O. K. Andersen, A. V. Postnikov, and S. Yu Savrasov, in *Application of Multiple Scattering Theory to Materials Science*, edited by W. H. Butler, P. H. Dederichs, A. Gonis, and R. L. Weaver, MRS Symposia Proceedings No. 253 (Materials Research Society, Pittsburgh, 1992).
[17] O. K. Andersen and O. Jepsen, Phys. Rev. Lett. **53**, 2571 (1984).
[18] O. K. Andersen, O. Jepsen, and G. Krier, in *Lectures on Methods of Electronic Structure Calculations*, edited by V. Kumar, O. K.

Andersen, and A. Mookerjee (World Scientific, Singapore, 1994).
[19] R. Zeller, P. H. Dederichs, B. Újfalussy, L. Szunyogh, and P. Weinberger, Phys. Rev. B **52**, 8807 (1995).
[20] R. Zeller, J. Phys. C **20**, 2347 (1987).
[21] R. G. Newton, Phys. Rev. Lett. **65**, 2031 (1990).
[22] W. H. Butler, A. Gonis, and X.-G. Zhang, Phys. Rev. B **45**, 11 527 (1992); **48**, 2118 (1993).
[23] S. Bei der Kellen, Y. Oh, E. Badralexe, and A. J. Freeman, Phys. Rev. B **51**, 9560 (1995).
[24] J. M. Ziman, in *Solid State Physics: Advances in Research and Applications*, edited by H. Ehrenreich, F. Seitz, and D. Turnbull (Academic Press, New York, 1971), Vol. 26, p. 1.
[25] F. S. Ham and B. Segall, Phys. Rev. **124**, 1786 (1961).
[26] P. E. Blöchl, O. Jepsen, and O. K. Andersen, Phys. Rev. B **49**, 16 223 (1994).
[27] J. J. Dongarra and D. W. Walker, SIAM Rev. **37**, 151 (1995).
[28] B. Drittler, M. Weinert, R. Zeller, and P. H. Dederichs, Solid State Commun. **79**, 31 (1991).
[29] N. Stefanou, H. Akai, and R. Zeller, Comput. Phys. Commun. **60**, 231 (1990).
[30] D. M. Ceperley and B. J. Alder, Phys. Rev. Lett. **49**, 566 (1980).
[31] S. H. Vosko, L. Wilk, and M. Nusair, Can. J. Phys. **58**, 1200 (1980).
[32] R. Zeller, J. Deutz, and P. H. Dederichs, Solid State Commun. **44**, 993 (1982).
[33] K. Wildberger, P. Lang, R. Zeller, and P. H. Dederichs, Phys. Rev. B **52**, 11 502 (1995).
[34] R. Zeller, in *Electronic Properties of Solids Using Cluster Methods*, edited by T. A. Kaplan and S. D. Mahanti (Plenum Press, New York, 1995), p. 41.
[35] J. Birch, J. Geophys. Res. **83**, 1257 (1978).
[36] I. S. Duff, A. M. Erisman, and J. K. Reid, *Direct Methods for Sparse Matrices* (Clarendon Press, Oxford, 1986).
[37] *Iterative Methods for Large Linear Systems*, edited by D. R. Kincaid and L. J. Hayes (Academic Press, Boston, 1990).
[38] K. Wildberger, R. Zeller, and P. H. Dederichs, Phys. Rev. B (to be published).
[39] R. Haydock, in *Solid State Physics: Advances in Research and Applications*, edited by H. Ehrenreich, F. Seitz, and D. Turnbull (Academic Press, New York, 1980), Vol. 35, p. 215.
[40] N. Chetty, M. Weinert, T. S. Rahman, and J. W. Davenport, Phys. Rev. B **52**, 6313 (1995).
[41] M. Methfessel, Phys. Rev. B **52**, 8074 (1995).
[42] J. Choi, J. Demmel, I. Dhillon, J. Dongarra, S. Ostrouchov, A. Petitet, K. Stanley, D. Walker, and R. C. Whaley, Comput. Phys. Commun. **97**, 1 (1996).
[43] R. Zeller, Int. J. Mod. Phys. C **4**, 1109 (1993).